2013

Enhanced hemangioblast generation and improved vascular repair and regeneration from embryonic stem cells by defined transcription factors

Fang Liu
Washington University School of Medicine in St. Louis

Suk Ho Bhang
Washington University School of Medicine in St. Louis

Elizabeth Arentson
Washington University School of Medicine in St. Louis

Atsushi Sawada
Washington University School of Medicine in St. Louis

Chan Kyu Kim
Washington University School of Medicine in St. Louis

See next page for additional authors

Stem Cell Reports
Article

ISSCR

OPEN ACCESS

Enhanced Hemangioblast Generation and Improved Vascular Repair and Regeneration from Embryonic Stem Cells by Defined Transcription Factors

Fang Liu,[1,6] Suk Ho Bhang,[2,6,9] Elizabeth Arentson,[1] Atsushi Sawada,[3] Chan Kyu Kim,[1,7] Inyoung Kang,[1,4] Jinsheng Yu,[5] Nagisa Sakurai,[1] Suk Hyung Kim,[1,8] Judy Ji Woon Yoo,[2] Paul Kim,[2] Seong Ho Pahng,[2] Younan Xia,[2,9] Lilianna Solnica-Krezel,[3,4] and Kyunghee Choi[1,4,*]

[1]Department of Pathology and Immunology
[2]Department of Biomedical Engineering
[3]Department of Developmental Biology
[4]Developmental, Regenerative, and Stem Cell Biology Program
[5]Department of Genetics
Washington University School of Medicine, St. Louis, MO 63110, USA
[6]These authors contributed equally to this work
[7]Present address: Soonchunhyang University School of Medicine, Seoul, Korea
[8]Present address: Samsung Research Institute, Seoul, Korea
[9]Present address: Department of Biomedical Engineering, Georgia Institute of Technology, Atlanta, GA 30332, USA
*Correspondence: kchoi@wustl.edu
http://dx.doi.org/10.1016/j.stemcr.2013.06.005

SUMMARY

The fetal liver kinase 1 (FLK-1)$^+$ hemangioblast can generate hematopoietic, endothelial, and smooth muscle cells (SMCs). ER71/ETV2, GATA2, and SCL form a core transcriptional network in hemangioblast development. Transient coexpression of these three factors during mesoderm formation stage in mouse embryonic stem cells (ESCs) robustly enhanced hemangioblast generation by activating bone morphogenetic protein (BMP) and FLK-1 signaling while inhibiting phosphatidylinositol 3-kinase, WNT signaling, and cardiac output. Moreover, *etsrp*, *gata2*, and *scl* inhibition converted hematopoietic field of the zebrafish anterior lateral plate mesoderm to cardiac. FLK-1$^+$ hemangioblasts generated by transient coexpression of the three factors (ER71-GATA2-SCL [EGS]-induced FLK-1$^+$) effectively produced hematopoietic, endothelial, and SMCs in culture and in vivo. Importantly, EGS-induced FLK-1$^+$ hemangioblasts, when codelivered with mesenchymal stem cells as spheroids, were protected from apoptosis and generated functional endothelial cells and SMCs in ischemic mouse hindlimbs, resulting in improved blood perfusion and limb salvage. ESC-derived, EGS-induced FLK-1$^+$ hemangioblasts could provide an attractive cell source for future hematopoietic and vascular repair and regeneration.

INTRODUCTION

Pluripotent stem cells provide an exciting opportunity in the field of basic as well as regenerative biology because of their unique capacity to differentiate in culture into all somatic cells that form an individual. Current efforts are aimed at generating a preferred somatic cell type by manipulating growth factors added to culture media. While these efforts have advanced the field, derivation of a homogenous specific cell population from embryonic stem cells (ESCs) or induced pluripotent stem cells (iPSCs) still remains as a major challenge in the field. Successful derivation of a desired somatic cell lineage from ESCs or iPSCs would likely to be advanced by comprehensive understanding of how specification of that particular cell lineage is accomplished in the developing embryo. As for blood and vessel development, tracking a receptor tyrosine kinase fetal liver kinase 1 (FLK-1) expression has been instrumental. Specifically, cell lineage tracing studies have demonstrated that FLK-1$^+$ mesoderm contributes to primitive and definitive blood, endothelial cells, and cardiac and skeletal muscles (Lugus et al., 2009; Motoike et al., 2003). FLK-1$^+$ (or KDR$^+$ in human) mesoderm isolated from ESCs or embryos can generate hematopoietic, endothelial, and smooth muscle cells as well as cardiac cells (Choi et al., 1998; Faloon et al., 2000; Yamashita et al., 2000; Ema et al., 2003; Huber et al., 2004; Kennedy et al., 2007; Kattman et al., 2006; Moretti et al., 2006; Yang et al., 2008). Importantly, hemangiogenic or cardiogenic potential of the FLK-1$^+$ mesoderm can be segregated by the platelet-derived growth factor receptor α (PDGFRα) expression in both mouse and human, such that, while the FLK-1$^+$PDGFRα$^-$ cell population is enriched for the hemangiogenic potential, FLK-1$^+$PDGFRα$^+$ cell population is enriched for the cardiogenic potential (Kattman et al., 2011; Liu et al., 2012).

Molecularly, there is an antagonistic relationship between the hemangiogenic and cardiogenic mesodermal outcome. For example, enforced *Er71* expression leads to an increase in hematopoietic and endothelial cell output but a decrease in cardiac output. Conversely, *Er71* deficiency results in defective hematopoietic and endothelial cell output but enhanced cardiac outcome (Lee et al., 2008; Liu et al., 2012). Similarly, the hematopoietic program is inhibited

by enforced Mesp1 or Nkx2-5 expression, which promotes cardiac differentiation (Caprioli et al., 2011; Lindsley et al., 2008).

Herein, we reasoned that hemangioblast generation from ESCs could be enhanced by inhibiting cardiac output with defined hemangiogenic factors. We presumed that the candidate factors should be preferentially expressed within the hemangioblast population, that they could individually skew toward the hemangiogenic output, and that the skewing effect could be most dramatic when the candidate factors were coexpressed. We identify ER71, GATA2, and SCL as core factors in hemangioblast development. Transient coexpression of these three factors during mesoderm formation stage robustly enhanced FLK-1$^+$ hemangioblast (FLK-1$^+$PDGFRα$^-$) production while concomitantly inhibiting cardiac outcome from differentiating ESCs. Such FLK-1$^+$ hemangioblasts generated functional endothelial and smooth muscle cells in culture as well as in ischemic mouse hindlimbs, resulting in improved blood perfusion and limb salvage.

RESULTS

FLK-1$^+$PDGFRα$^-$ Cells from ESCs Can Be Potently Generated by Temporal ER71, GATA2, and SCL Coexpression

We previously reported gene expression profiling of the presumptive hemangioblasts, FLK-1$^+$SCL$^+$ (Chung et al., 2002; Lugus et al., 2007). Focusing on the genes that were preferentially expressed within FLK-1$^+$SCL$^+$ cells or FLK-1$^+$ cells (Figure S1A available online), we determined if any of these could skew mesoderm toward the hemangiogenic FLK-1$^+$PDGFRα$^-$ outcome from ESCs. To this end, we generated A2 ESCs expressing single candidate genes in a doxycycline (DOX)-inducible manner (Ismailoglu et al., 2008). We induced candidate genes from day 2 and analyzed FLK-1 and PDGFRα expression between days 3 and 4, mesoderm formation, and patterning stage. While the majority of the candidate genes did not show skewing potential, we could detect skewing outcome toward FLK-1$^+$PDGFRα$^-$ mesoderm with *Er71*-, *Gata2*-, or *Scl*-enforced expression (Figures 1A, S2A, and S2B). Parent A2 or other ESC line R1 showed similar differentiation potential generating FLK-1$^+$ and/or PDGFRα$^+$ cells (Figure S1B), indicating that genetic manipulation did not alter the differentiation potential of the A2 ESCs.

Of the three factors, enforced *Er71* expression readily generated FLK-1$^+$PDGFRα$^-$ cells as early as day 3. However, the FLK-1$^+$ PDGFRα$^-$ skewing effect was not effectively maintained at later time points, as we could detect PDGFRα expression on day 4 (Figure 1A). Enforced *Scl* expression resulted in slightly different kinetics, such that FLK-1$^+$PDGFRα$^-$ cells were most abundant at a later time point, day 4. Enforced *Gata2* expression appeared to mainly suppress FLK-1$^+$PDGFRα$^+$ cells without significant increase in FLK-1$^+$PDGFRα$^-$ cells. As the analyses of the enforced *Er71*, *Gata2*, or *Scl* expression suggested that these three factors might function synergistically, we next determined if temporal coexpression of these three factors were even more powerful in the skewing effect. Thus, we generated A2 ES cells coexpressing *Er71*, *Gata2*, and *Scl* in a DOX-inducible manner. Notably, only the FLK-1$^+$PDGFRα$^-$ cells, not FLK-1$^+$PDGFRα$^+$ nor PDGFRα$^+$, in both serum (Figure 1A) and serum-free conditions (Figure 4E) were generated when we coexpressed the three factors. FLK-1$^+$PDGFRα$^+$ cells were still suppressed at day 4. Hematopoietic and endothelial cell transcription factor and surface receptor genes were strongly upregulated in these FLK-1$^+$PDGFRα$^-$ cells (Figure 1B). On the other hand, cardiac transcription factors, including *Mesp1* and *Islet1* as well as *Pdgfrα* genes, were greatly suppressed in these FLK-1$^+$PDGFRα$^-$ cells. Collectively, temporal coexpression of *Gata2* and *Scl* together with *Er71* results in the most powerful effect generating FLK-1$^+$PDGFRα$^-$ cells.

ER71, GATA2, and Scl-Induced Hemangioblast Can Further Differentiate into Hematopoietic and Endothelial Cells In Vitro and In Vivo

To determine if FLK-1$^+$PDGFRα$^-$ cells generated by the transient *Er71*, *Gata2*, and *Scl* coexpression, designated as ER71-GATA2-SCL (EGS)-induced FLK-1$^+$, were enriched for "bona fide" hemangioblasts, we subjected day 3 embryoid body (EB) cells, control and DOX-treated, to blast colony assay, an in vitro measure of hemangioblast (Choi et al., 1998). Remarkably, DOX-treated EB cells, compared to controls, generated greatly enhanced number of blast colonies (Figure 1C). More importantly, blast colonies were readily generated with DOX from serum-free conditions plus bone morphogenetic protein 4 (BMP-4), which normally do not support blast colony formation (Figures 1D and 1E). To determine if indeed all blast colonies developed from FLK-1$^+$ cells, we sorted FLK-1$^+$ cells from day 3 EBs, control and DOX-treated, and subjected to blast colony assay. Again, FLK-1$^+$PDGFRα$^-$ cells generated from DOX-treated EBs produced an increased blast colony number compared to control FLK-1$^+$ cells (Figure 1F). Blast cells are capable of generating blood, endothelial, and smooth muscle cells (Choi et al., 1998; Ema et al., 2003; Yamashita et al., 2000). To further validate that the differentiation potential of blast colonies generated from EGS-induced FLK-1$^+$ cells were the same as the controls, we subjected individual blast colonies to further differentiation into hematopoietic, endothelial, and smooth muscle cells. Similar percentage of blast colonies from control and DOX-treated EBs generated both hematopoietic and adherent cells (Figure S1C). Adherent cells contained both CD31$^+$ (or VE-CADHERIN$^+$)

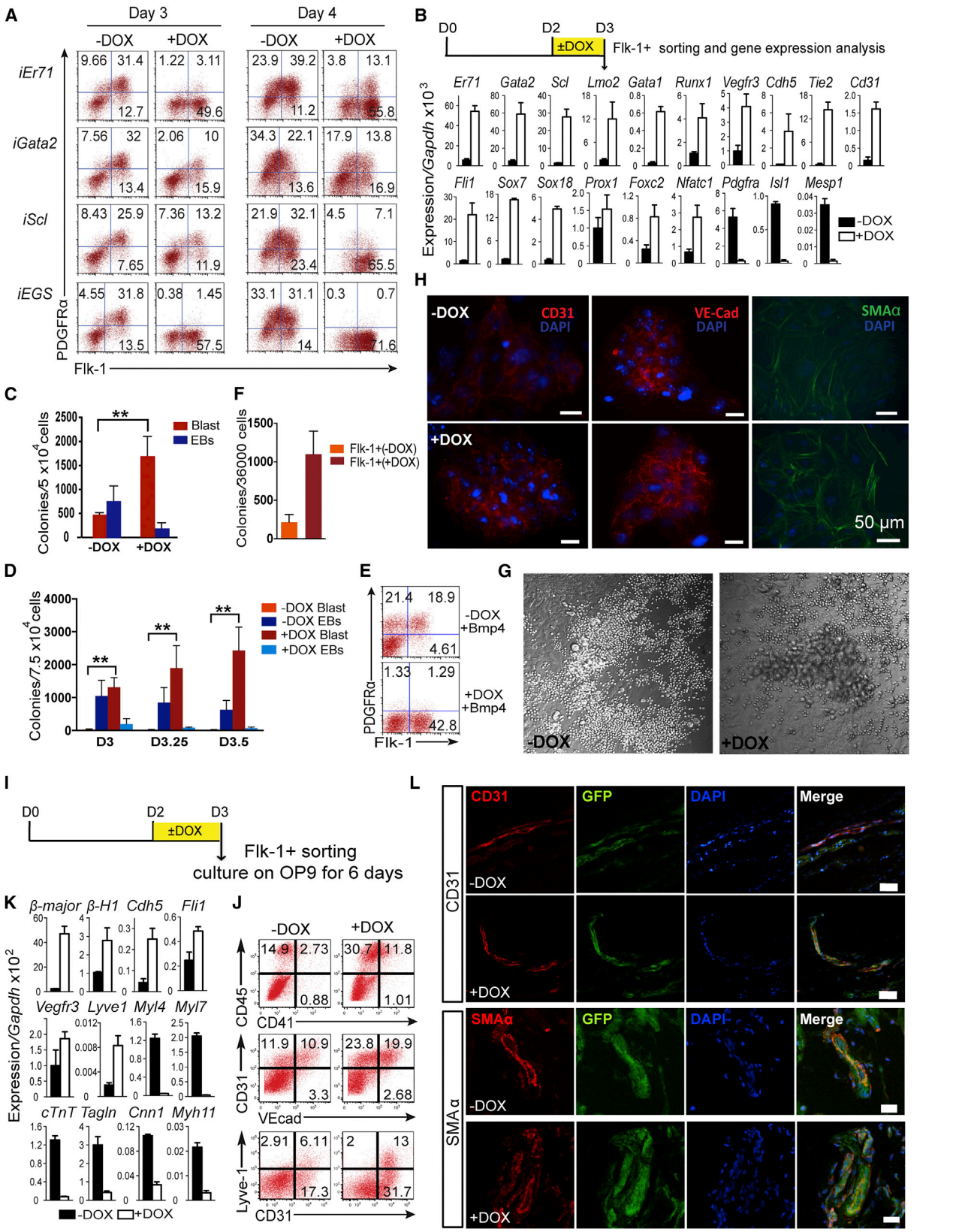

(legend on next page)

and SMA-α^+ cells, indicating that DOX treatment resulted in enhanced hemangioblast generation without altering their differentiation potential (Figures 1G, 1H, and S1D).

As expected, FLK-1$^+$ cells, control and DOX-treated, robustly generated hematopoietic (CD45$^+$ and CD41$^+$) and endothelial (VE-CADHERIN$^+$ and CD31$^+$) cells when cultured on OP9 cells (Figure 1J and S1E). Gene expression analyses also corroborated with cell surface marker studies (Figure 1K). Lymphatic endothelial cell marker genes, including *Prox1*, *Vegfr3*, and *Lyve1*, were also highly expressed in EGS-induced FLK-1$^+$ and differentiated progeny cells (Figures 1B, 1J, and 1K).

Functional hematopoietic and endothelial cell outcome from EGS-induced FLK-1$^+$ cells was further determined in vivo by Matrigel plug assay. Control FLK-1$^+$ or EGS-induced, FLK-1$^+$-derived GFP$^+$CD31$^+$ as well as GFP$^+$SMA-α^+ cells were detected (Figures 1L, S1F, and S1G). The occurrence of GFP$^+$CD45$^+$ cells was more frequent from Matrigel plugs obtained from EGS-induced FLK-1$^+$ cells (Figures 1L, S1G, and S1H). In some cases, such vessels were filled with round GFP$^+$ but DAPI negative cells, suggesting these cells could be mature erythrocytes derived from FLK-1$^+$ hemangioblasts (Figure S1G). Collectively, FLK-1$^+$ cells, control or EGS-induced, contain functional progenitors for hematopoietic, endothelial, and smooth muscle cells. EGS-induced FLK-1$^+$ cells are highly effective in generating blood, endothelial cells, and smooth muscle cells in vivo.

etsrp, *gata2*, and *scl* Inhibition Can Successfully Convert the Hematopoietic Field of the Zebrafish Anterior Lateral Plate Mesoderm to a Cardiac Field

To further ascertain that cardiogenic versus hemangiogenic outcome can be manipulated by the three hemangiogenic transcription factors, we determined if the cardiac field can be extended by suppressing *er71*, *gata2*, and *scl* expression in zebrafish. Fate-mapping studies in zebrafish have established that, while blood and endothelial cells originate from the rostral part of the anterior lateral plate mesoderm (ALPM), cardiac cell lineages originate from the medial and lateral parts (Figures 2A and 2B; Schoenebeck et al., 2007). Moreover, limiting blood and vessel specification resulted in expansion of cardiac progenitors (Schoenebeck et al., 2007). We observed that *etsrp* morpholino (MO) injection alone was sufficient to convert the hemangiogenic field to cardiac, as evidenced by *hand2* expression in the rostral part (Figure 2C), with concomitant loss of *fli1a* expression, a gene critical for the hemangioblast specification in zebrafish (Liu et al., 2008). This effect was specific to the ALPM, as the lateral *fli1* expression was not affected (Figure 2K). More importantly, *etsrp*-deficient embryos readily expressed *hand2* in the rostral region of the ALPM (Figure 2D). *scl* MO injection also resulted in a similar extension of the cardiac field (Figure 2E). Although *gata2* MO did not extend *hand2* expression rostrally, the *hand2* expression domain was expanded within the medial/lateral part (Figure 2F). Whereas ~75% of wild-type embryos coinjected with

Figure 1. Enhanced FLK-1$^+$PDGFRα^- Hemangioblast Generation by Temporal *Er71*, *Gata2*, and *Scl* Coexpression

(A) *iEr71*, *iGata2*, *iScl*, or *iEGS* (= *iEr71-2A-Gata2-2A-Scl*) EBs were treated with DOX from day 2 and analyzed for FLK-1 and PDGFRα at indicated times. Numbers indicate the percentage of live cells gated within each quadrant. Representative results from four independent experiments are shown.

(B) FLK-1$^+$ cells were sorted from day 3 *iEGS* EBs (±DOX from day 2) and analyzed for gene expression. Expression levels relative to *Gapdh* are shown as mean ± SD of three independent experiments.

(C and F) Day 3 *iEGS* EBs (±DOX from day 2) were subjected to blast colony assay. Colony numbers are shown as mean ± SD of four independent experiments $^{**}p < 0.01$, compared to −DOX.

(D) *iEGS* ESCs were differentiated in serum-free conditions with BMP-4 (10 ng/ml) and DOX added from day 0 and day 2, respectively, and replated on day 3, 3.25, or 3.5. Blast colonies and secondary EBs were counted on day 4. Colony numbers are shown as mean ± SD of four independent experiments, $^{**}p < 0.01$, compared to −DOX.

(E) *iEGS* ESCs were differentiated as in (D) and analyzed for FLK-1 and PDGFRα on day 3.5.

(F) FLK-1$^+$ cells sorted from day 3 *iEGS* EBs (±DOX from day 2) were subjected to blast colony assay. Colony numbers are shown as mean ± SD of four independent experiments $^{**}p < 0.01$, compared to −DOX.

(G and H) Individual blast colonies were picked and cultured on type IV collagen-coated microtiter well in the presence of cytokines. Bright-field images of hematopoietic and adherent cells are shown (G), scale bar: 50 μm. After removing hematopoietic cells, adherent cells were immunostained for CD31 (red), VE-CADHERIN (red), SMAα (green), and DAPI nuclear staining (blue) (H). Scale bar: 20 μm for CD31 and VE-CADHERIN; 50 μm for SMAα.

(I–K) FLK-1$^+$ cells were sorted from day 3 *iEGS* EBs (±DOX from day 2), cultured on OP9 cells for 6 days, and fluorescence-activated cell sorting-analyzed for CD41, CD45, CD31, LYVE-1, and VE-CADHERIN (J) or gene expression (K). Expression levels relative to *Gapdh* are shown as mean ± SD of three independent experiments.

(L) FLK-1$^+$ cells were sorted as in (I), infected with GFP retrovirus, mixed in with OP9 cells and Matrigel, and injected subcutaneously into nonobese diabetic/severe combined immunodeficiency/interleukin 2 Rγ−/− mice. After 2 weeks, Matrigel plugs were excised and assessed for GFP+CD31+ or GFP+SMAα+ by immunostaining. Nuclei are shown in blue with DAPI (scale bar: 50 μm).

See also Figures S1 and S2 and Table S2.

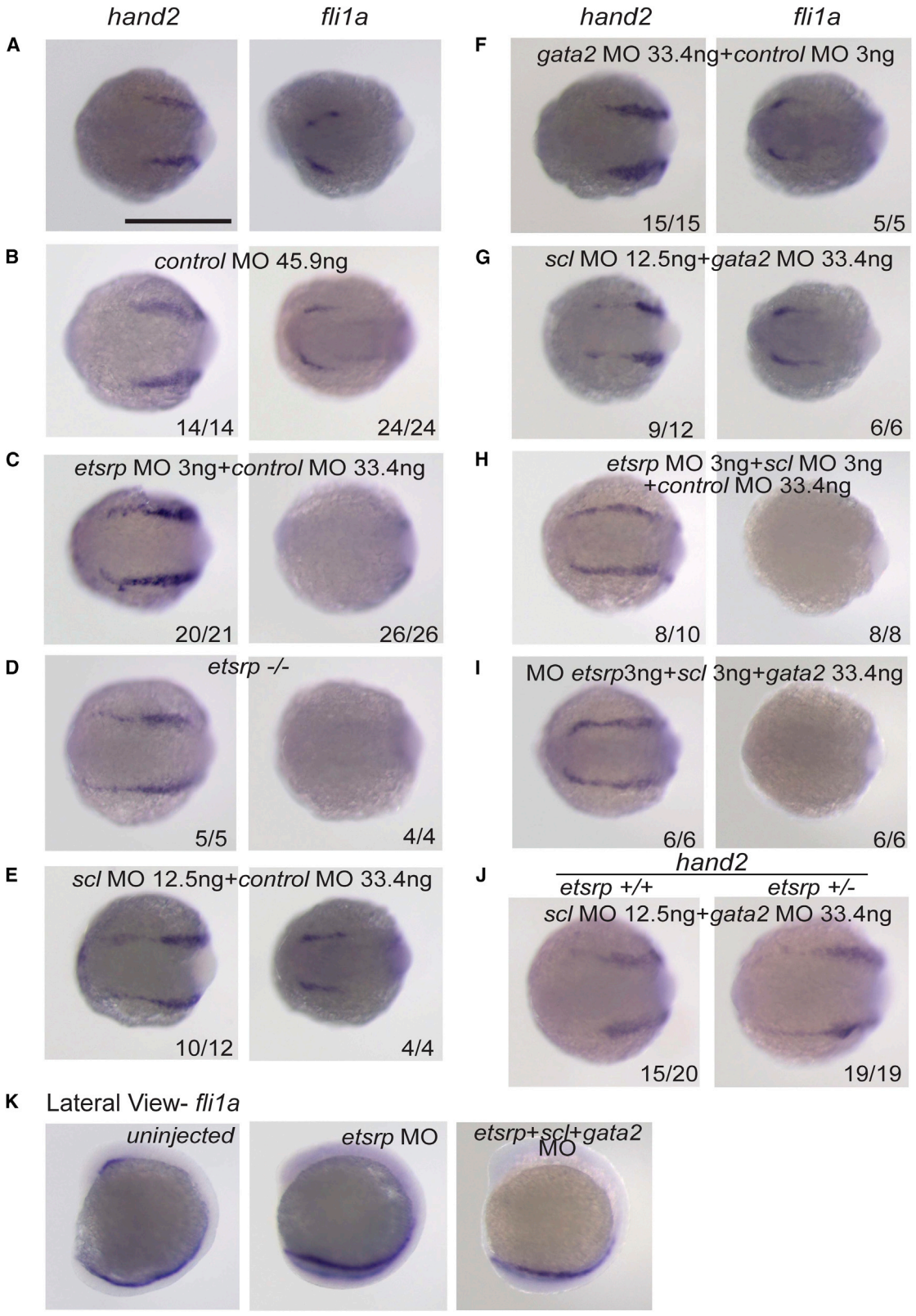

(legend on next page)

gata2 and *scl* MOs displayed the rostral extension of *hand2* expression, 100% of the *etsrp* heterozygous (*etsrp*$^{y1\ 1/+}$) embryos (Pham et al., 2007), coinjected with these two MOs showed anterior enlargement of *hand2* expression (Figures 2G and 2J). Importantly, while ~80% of embryos coinjected with *etsrp* and *scl* MO resulted in rostral *hand2* extension, 100% of the embryos showed conversion of the hemangiogenic field to cardiac when coinjected with all three MOs (Figures 2H and 2I). These results suggest the cooperativity among *Er71*, *Scl*, and *Gata2* in promoting hemangiogenic mesoderm development. Collectively, simultaneous modulation of *Er71*, *Gata2*, and *Scl* expression in ESC or zebrafish has profound effect on the hemangiogenic outcome.

ER71, GATA2, and SCL-Mediated Genetic Program in Hemangioblast Development

The earlier and robust effect of *Er71*, compared to *Gata2* or *Scl*, on the FLK-1$^+$ PDGFRα^-, skewing both in ESC and zebrafish models, suggested that ER71 functions upstream of GATA2 and SCL. Indeed, we previously reported that *Er71* expression in embryos and EBs is transient (Lee et al., 2008). The onset of *Er71* expression in wild-type EBs precedes that of *Gata2* and *Scl* expression (Figure S3A). Moreover, *Gata2* or *Scl* expression in EBs was not detected in the absence of ER71 (Figure S3A). We also detected ER71 occupancy on the *Scl* promoter region (Figure S4). Moreover, *Er71*-enforced expression resulted in robust *Gata2* and *Scl* upregulation. On the other hand, *Gata2* or *Scl*-enforced expression failed to upregulate *Er71* expression (Figure S3B). We conclude that ER71 establishes *Gata2* and *Scl* expression during hemangioblast development.

To better understand genetic program-regulating hemangioblast formation, we compared global temporal gene expression changes by enforced ER71, GATA2, and Scl coexpression. Specifically, we saw an upregulation of *Er71, Gata2*, and *Scl* expression by 6 hr after DOX addition, indicating that 6 hr DOX treatment was sufficient to induce these exogenous genes. Thus, RNA from day 2.25 (6 hr after DOX addition), day 2.5 (12 hr after DOX addition), and day 3 (24 hr after DOX addition) EB cells was subjected to microarray analyses. Notably, *Fli-1, Lmo2, Esam, Sox7, Sox18, Hey1, Flk-1*, and *Cdh5* expression was significantly upregulated within 6 hr after DOX addition, suggesting that these genes are presumably direct targets of ER71, GATA2, and Scl (Figures 3A and 3B). Indeed, we previously demonstrated that *Flk-1* and *Ve-cadherin/Cdh5* are ER71 direct targets (Lee et al., 2008; Liu et al., 2012). Recent studies have reported that *Lmo2* is also an ER71 direct target (Koyano-Nakagawa et al., 2012). While hematopoietic and endothelial cell genes became progressively upregulated over the course of 24 hr DOX treatment, cardiac genes, including *Hand1, Isl1*, and *Mesp1*, were progressively downregulated within the same time frame (Figures 3A and 3B). At the same time, *Flk-1* expression and downstream signaling pathway genes were greatly upregulated by 24 hr after DOX addition (Figures 3C–3E). Cell adhesion molecules as well as *Bmp-4* and *Bmp-6* were also upregulated. On the other hand, BMP-4 inhibitors, including *Follistatin* and *Cer-1* gene expression, were greatly inhibited. WNT signaling and epithelial-mesenchymal transition (EMT) pathway genes were also significantly downregulated (Figures 3C–3E; Table S1). Collectively, our data suggested that enforced *Er71*, *Gata2*, and *Scl* coexpression resulted in activation of BMP and FLK-1 signaling and inhibition of EMT and WNT signaling.

We further performed biochemical analyses to confirm the signaling pathways identified by the global gene expression profiling. DOX treatment resulted in an increase of the total SMAD1/SMAD5/SMAD8 protein levels as well as a significant enhancement of phospho-SMAD1/SMAD5/SMAD8, indicating that BMP signaling was indeed activated (Figure 4A). AKT/protein kinase B (AKT) phosphorylation was greatly reduced, but ERK phosphorylation was strongly enhanced by DOX treatment (Figure 4A). As total AKT or ERK protein levels remained the same, ER71, GATA2, and SCL induce hemangioblasts by selectively activating the map kinase pathway. Phopho-glycogen synthase kinase 3β (GSK3β) levels at serine 9 were greatly decreased upon DOX treatment (Figure 4A). The total amount of GSK3β remained the same. DOX treatment also resulted in lymphoid enhancer-binding factor-1 (LEF1) inhibition (Figure 4A), a key component in WNT target gene expression. Potentially, ER71-, GATA2-, and SCL-mediated WNT inhibition is achieved both by GSK-3β-βCATENIN as well as LEF1 inhibition. As for EMT,

Figure 2. Combinatorial Suppression of *er71/etsrp*, *gata2*, and *scl* Promotes Cardiogenic Output in Zebrafish Anterior Lateral Plate Mesoderm

(A–I) In situ hybridization depicts *hand2* and *fli1a* expression in uninjected (A), control (B), and *etsrp* MO embryos (C; 3 ng), *scl* MO (E; 12.5 ng), *gata2* MO (F; 33.4 ng), *gata2* (33.4 ng)+*scl* (12.5 ng) MOs (G), *etsrp* (3 ng)+*scl* (3 ng) MOs (H), *etsrp* (3 ng)+*scl* (3 ng)+*gata2* (33.4 ng) MOs (I)-injected embryos, and *etsrp*−/− embryos (D).

(J) Expression of *hand2* in *gata2* (33.4 ng)+*scl* (12.5 ng) MOs-injected *etsrp*+/+ and *etsrp*+/− embryos. The numbers show the severe phenotype. (A–J) Seven-somite stage, dorsal views, anterior to the left.

(K) Lateral view of *flia* expression in uninjected, *etsrp* MO, or *etsrp+scl+gata2* MO-injected embryos. Scale bar: 500 μm.

See also Table S4.

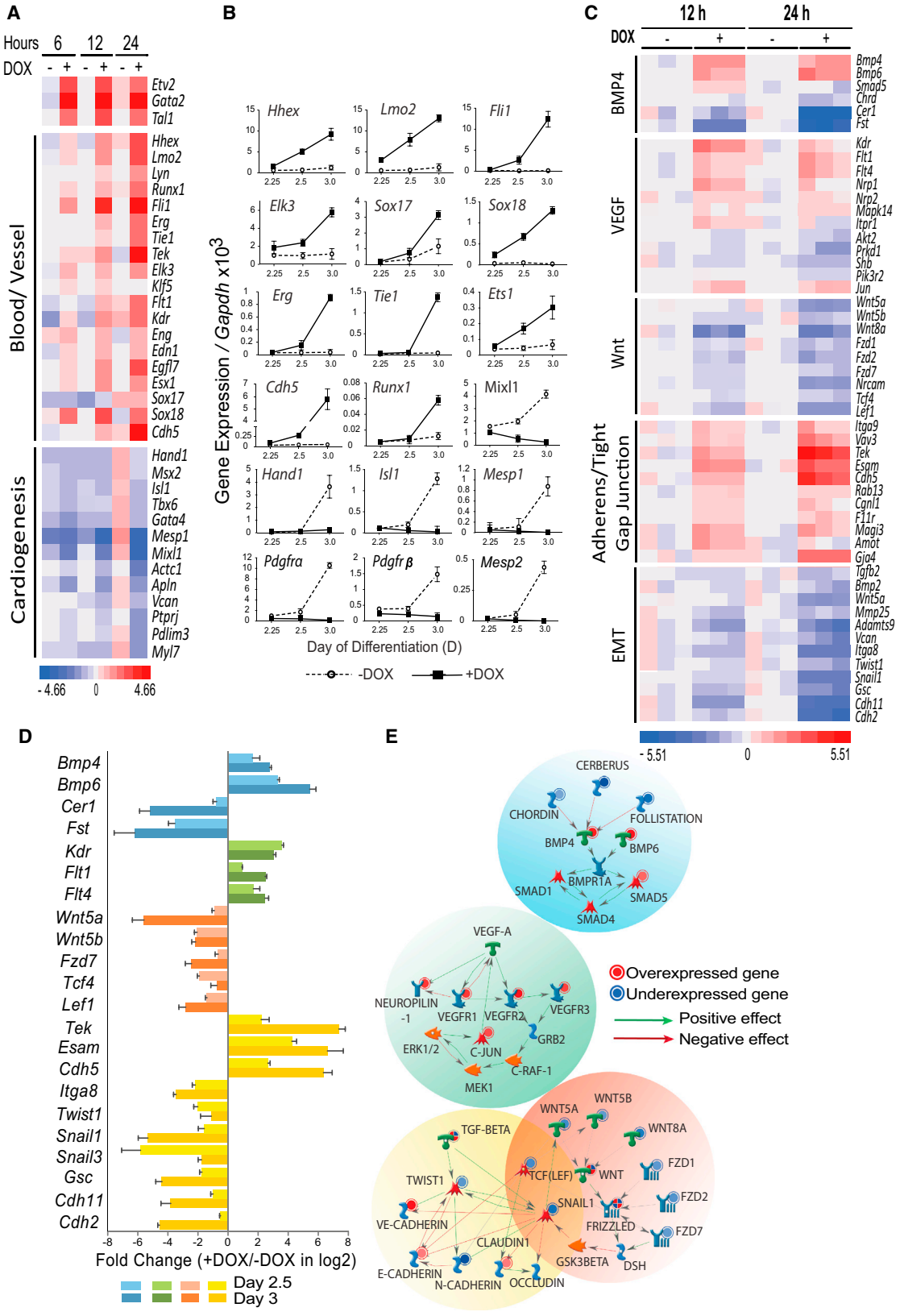

(legend on next page)

DOX treatment (from day 2 or 3) greatly suppressed N-CADHERIN expression (Figure 4B). At the same time, genes involved in EMT processes, including *Snail1* and *Twist1*, were also suppressed by DOX addition (Figure 4C). CHIR99021, a GSK3β inhibitor, could partially rescue *Snail1* inhibition by DOX treatment (Figure 4D) but not *Mesp1* suppression or FLK-1$^+$PDGFRα$^+$ cardiac mesoderm (not shown). Notably, activation of the map kinase pathway and inhibition of the phosphatidylinositol 3-kinase (PI3K)/AKT pathway was readily observed by enforced *Er71* expression alone. SMAD1/SMAD5 activation and WNT inhibition was readily observed by enforced *Gata2* and *Scl* expression, respectively (Figure 4A). This suggested that ER71, GATA2, and SCL may distinctly contribute to hemangioblast development, and the combined sum of ER71, GATA2, and SCL activity is required for the most efficient hemangioblast generation.

Since the PI3K pathway appeared to negatively regulate hemangioblast formation, we tested if we could produce FLK-1$^+$PDGFRα$^-$ cells even more robustly by adding PI3K inhibitor. The percentage of FLK-1$^+$PDGFRα$^-$ cells generated was significantly higher when we added DOX and PI3K inhibitor together (Figure 4E). On the other hand, FLK-1$^+$PDGFRα$^-$ cells were generated less when a map kinase inhibitor was added together with DOX, indicating that the map kinase pathway positively regulates the FLK-1$^+$PDGFRα$^-$ cell formation (Figure 4E).

EGS-Induced FLK-1$^+$ Cells Can Potently Enhance Angiogenic Repair and Regeneration

We tested if ESC-derived, EGS-induced FLK-1$^+$ (= FLK-1$^+$(+DOX)) cells could be used for angiogenic repair and regeneration. Remarkably, mesenchymal stem cells (MSCs) delivered as spheroids were superior to single MSC cells in supporting vascular therapeutic activity in a mouse model of hindlimb ischemia, as they were protected from apoptosis and secreted higher levels of angiogenic factors (Bhang et al., 2012; Shim et al., 2012). Thus, we determined if MSCs could be used as vehicles for delivering EGS-induced FLK-1$^+$ cells. To this end, we used human MSCs (hMSCs; from female) to distinguish the contribution of EGS-induced FLK-1$^+$ cells and MSCs in angiogenic repair. We first evaluated if EGS-induced FLK-1$^+$ cells could be protected from apoptosis while preserving endothelial differentiation potential by coculturing with hMSCs as spheroids. Specifically, spheroids generated between EGS-induced FLK-1$^+$ and hMSCs in different ratios (1:1, 1:5, and 1:10) were analyzed for the best condition that gave maximal cell survival of EGS-induced FLK-1$^+$ cells after switching to hypoxia (1% oxygen) to mimic an in vivo ischemic environment. EGS-induced FLK-1$^+$ cells under hypoxia readily became apoptotic when cocultured with hMSCs as single cells (Figures 5A and 5B). Spheroids containing only EGS-induced FLK-1$^+$ cells also displayed multiple apoptotic cells (Figures 5A and 5B). However, EGS-induced FLK-1$^+$ cells displayed significantly enhanced survival when cocultured with hMSCs as spheroids (Figures 5A and 5B). Consistently, while *Bcl-2* expression was readily detectable in (FLK-1$^+$(+DOX)+hMSC) spheroids, *p53* expression levels were high in single-cell culture or spheroids containing only FLK-1$^+$(+DOX) cells (Figures 5C, S5A, and S5B). Of the conditions, the 1:5 group showed the maximal cell viability. Mitochondrial metabolic activity was also significantly higher in the (FLK-1$^+$(+DOX)+hMSC) spheroids (1:5 ratio) compared to others (Figure S5C).

Previous studies have demonstrated that hMSCs readily upregulated hypoxia-inducible factor 1α (HIF-1α) in spheroids in hypoxia (Bhang et al., 2012; Shim et al., 2012). Consistently, HIF-1α expression was readily detected in (FLK-1$^+$(+DOX)+hMSC) spheroids, with the expression level being the highest in spheroids containing EGS-induced FLK-1$^+$ cells and hMSCs in a 1:5 ratio (Figures 5C, S5D, and S5E). HIF-1α upregulation resulted in

Figure 3. ER71, GATA2, and SCL-Mediated Genetic Program Regulating Hemangioblast Development

(A) Gene expression was assessed by microarray analysis at the indicated times (hr) after DOX addition. The average intensity for a given gene from three independent experiments is shown as heat map. Intensity values used in the heat maps are in log2 and normalized to mean of the −DOX samples. Red shading indicates increased expression, and blue shading indicates decreased expression.

(B) Kinetic expression levels of the indicated cell lineage markers over the time course of *iEGS* ESCs differentiation with (filled line) or without (dashed line) DOX is shown by qRT-PCR analysis. Data are presented as the mean values ± SD from four independent experiments.

(C) Heat map presents the relative expression of a subset of genes at the 12 and 24 hr after DOX addition implicated in the indicated pathways. Intensity values used in the heat maps are in log2 and normalized to mean of the −DOX samples at each time point. Data from three independent experiments are shown.

(D and E) Networks of the pathway regulation were created using MetaCore. (D) Fold-change of pathway genes in +DOX versus −DOX samples is shown. Data are presented as the mean values ± SD from three independent experiments. (E) Representative pathways that are focused on significantly affected interactions. Signaling pathways involved in BMP-4 is in blue; VEGF, green; WNT, brown; and EMT, yellow. Overlapping circles contain differentially expressed genes common to both pathways. Red solid circles indicate upregulated genes, and blue solid circles indicate downregulated genes. Green arrows show activation, and red arrows show suppression.

See also Figures S3 and S4 and Tables S1 and S2.

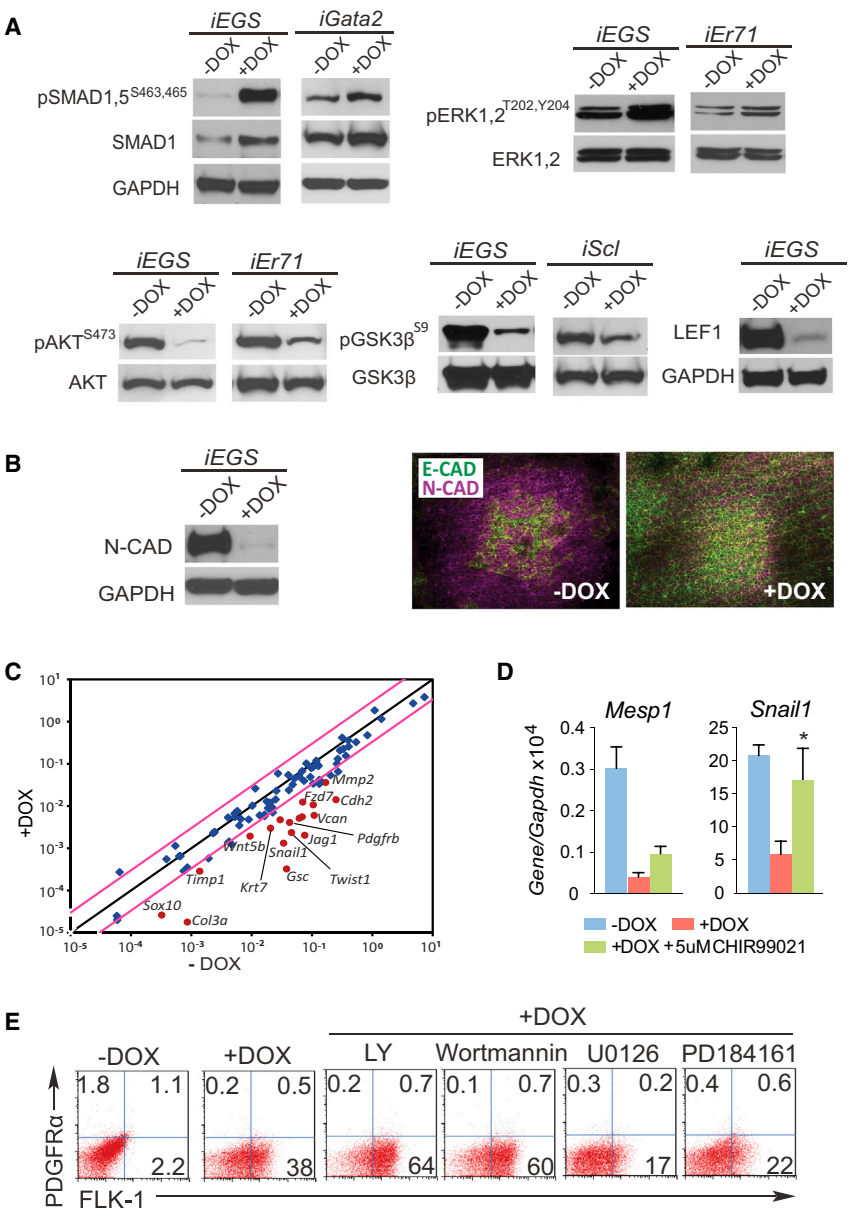

Figure 4. ER71, GATA2, and Scl-Mediated Signaling Pathways in Hemangioblast Development

(A) i*Er71*, i*Gata2*, i*Scl*, or *iEGS* ESCs were differentiated in serum-free conditions with DOX added from day 2. Day 4 EB-lysates were analyzed for signaling molecules by immunoblotting.

(B) *iEGS* EB cells were plated onto collagen I-coated slides on day 2 and stained with antibodies against E-CADHERIN (green) or N-CADHERIN (red) on day 4. N-CADHERIN protein expression levels in day 4 *iEGS* EBs (±DOX) are also shown by immunoblot analysis.

(C) Mouse EMT signaling SA-Bioscience QRT-PCR array on *iEGS* day 4 EBs (±DOX from day 2) are shown as scattered plots of fold changes normalized to three housekeeping genes for +DOX versus −DOX. Red dots are down-regulated genes in +DOX.

(D) iEGS ESCs were differentiated, CHIR99021 and DOX added from days 2–4, and analyzed for *Snail1* and *Mesp1* expression. Expression levels relative to *Gapdh* are shown as mean ± SD of three independent experiments. (The asterisk shows $p < 0.01$ compared to +DOX group).

(E) *iEGS* ESCs were differentiated in serum-free conditions, inhibitors and DOX added from day 2, and analyzed for FLK-1 and PDGFRα expression on day 4. PI3K inhibitors include LY294002 (10 μM) and Wortmannin (200 nM), MEK1/2 inhibitors include U0126 (10 μM) and PD184161 (10 μM).

See also Table S2.

enhanced human vascular endothelial growth factor (VEGF), basic fibroblast growth factor (bFGF), hepatocyte growth factor (HGF) gene expression, and protein production as measured by secreted protein levels. Angiogenic factor production was most robust in spheroids containing EGS-induced FLK-1$^+$ cells and hMSCs in a 1:5 ratio (Figures 5D, 5E, and S5F). Consequently, endothelial cells were efficiently generated in spheroids containing EGS-induced FLK-1$^+$ cells and hMSCs in a 1:5 ratio (Figures 5F and 5G). Spheroids containing only hMSCs did not express any endothelial cell genes (not shown). HIF-1α, mouse VEGF, or FGF expression was modest in spheroids generated with only EGS-induced FLK-1$^+$ cells (Figure 5C; data not shown). Vitronectin and laminin gene expression was efficiently induced in all spheroids, indicating that three-dimensional culture conditions augmented extracellular matrix protein production and cell-cell interactions (Figures 5H, S5G, and S5H). We conclude that ESC-derived, EGS-induced FLK-1$^+$ cells can be protected from hypoxia-induced apoptosis and further differentiate into endothelial cells when cocultured with MSCs as spheroids.

We assessed therapeutic efficacy of the (FLK-1$^+$(+DOX)+hMSC) spheroids in a mouse model of hind-limb ischemia. Specifically, we induced hind-limb ischemia in female nude mice, intramuscularly injected spheroids containing EGS-induced FLK-1$^+$ cells and hMSCs in a 1:5

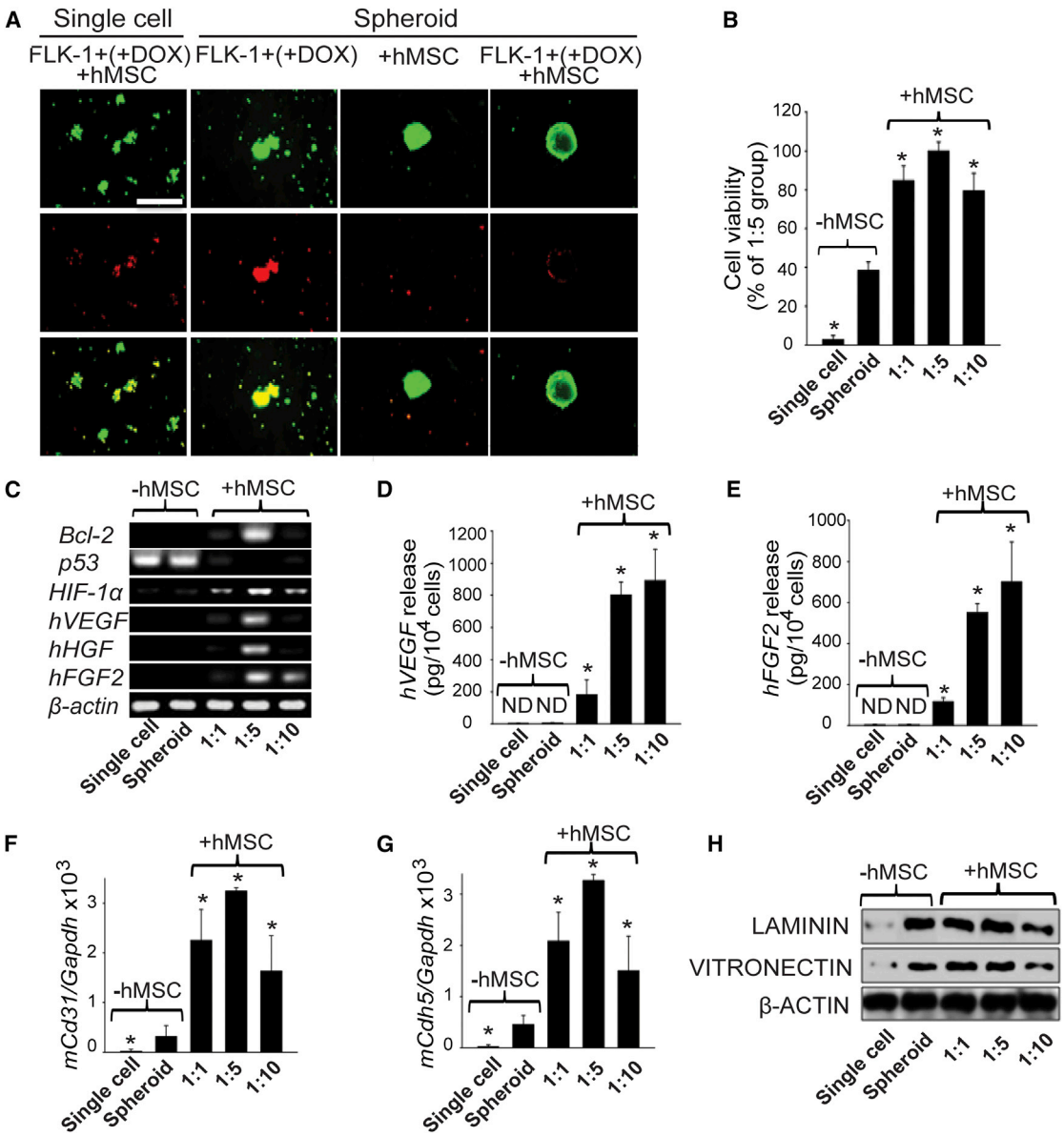

Figure 5. hMSCs Promote EGS-Induced FLK-1+ Cell Viability and Endothelial Cell Differentiation when Cocultured as Spheroids

Cells were cultured under hypoxic condition (1% oxygen).

(A and B) Cell viability was determined by fluorescein diacetate-ethidium bromide staining (A) (green: live cells; red: dead cells) or by neutral red assay (B) (*$p < 0.01$ compared to the FLK-1$^+$(+DOX) spheroid group; three independent experiments).

(C) RT-PCR analysis of *Bcl-2*, *p53*, hypoxia-inducible factor-1α, and angiogenic factors. Representative results from three independent experiments are shown.

(D and E) Angiogenic factors released from single cells and spheroids were determined by ELISA (*$p < 0.01$ compared to the FLK-1$^+$(+DOX) spheroid group; three independent experiments).

(F and G) Quantification of *Cd31* and *Cdh5* expression was determined by qRT-PCR. Expression levels relative to *Gapdh* are shown as mean ± SD of three independent experiments. The asterisk indicates $p < 0.01$ compared to the FLK-1$^+$(+DOX) spheroid group.

(H) Immunoblot analysis of extracellular matrices (LAMININ and VITRONECTIN).

See also Figure S5 and Table S2.

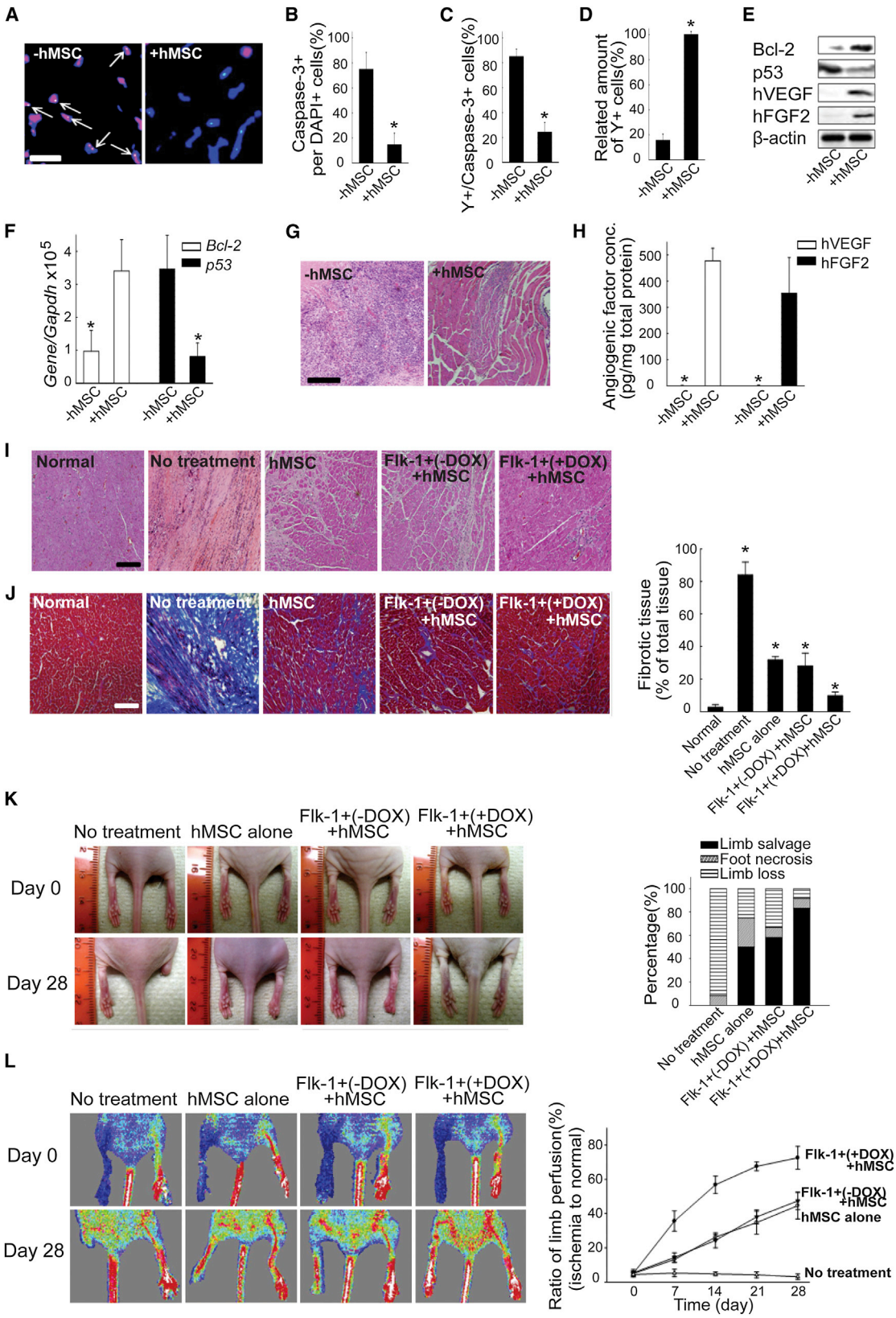

(legend on next page)

ratio (3×10^6 cells/limb, 5×10^5 EGS-induced FLK-1$^+$ cells + 2.5×10^6 hMSCs), and assessed the EGS-induced FLK-1$^+$ cell contribution to the recovery of the hind-limb ischemia by the presence of Y chromosome-positive cells (parent ESCs are male, XY). Three days after ischemia induction, the (FLK-1$^+$(+DOX)+hMSC) spheroid-recipient group contained significantly less caspase-3 and Y-positive cells (apoptotic cells, arrows) in the ischemic limb compared to the FLK-1$^+$(+DOX) spheroid-recipient group (Figures 6A–6C). Y-positive cells were more abundant in the (FLK-1$^+$(+DOX)+hMSC) spheroid-recipient group compared to the FLK-1$^+$(+DOX) spheroid-recipient group (Figure 6D). (FLK-1$^+$(+DOX)+hMSC) spheroid transplantation group displayed enhanced antiapoptotic gene expression (*Bcl-2*) and reduced proapoptotic factor (*p53*) gene expression (Figures 6E and 6F). Inflammation and muscle degeneration was attenuated in the (FLK-1$^+$(+DOX)+hMSC) spheroid-recipient group compared to that of FLK-1$^+$(+DOX) spheroid-recipient group, as judged by hematoxylin and eosin (H&E) staining (Figure 6G). Additionally, significant amount of human VEGF and FGF2 were detected in mouse ischemic tissues in the (FLK-1$^+$(+DOX)+hMSC) spheroid-recipient group compared to the FLK-1$^+$(+DOX) spheroid transplantation group (Figures 6E and 6H).

Twenty-eight days after ischemia induction, mice that received no treatment showed extensive muscle degeneration and inflammation in the ischemic region (Figures 6I and 6J), resulting in a complete limb loss (95.5%; n = 22) or severe limb necrosis (4.5%; Figure 6K). Mice that received FLK-1$^+$(+DOX) spheroids displayed similar muscle degeneration and limb loss (n = 5; data not shown). Mice that received hMSC spheroids did significantly better with decreased limb necrosis (Figure 6K). However, these mice still showed muscle degeneration and inflammation in the ischemic region (Figures 6I and 6J) and 27.3% of them ultimately lost limb (Figure 6K). Similar to mice that received hMSC spheroids, mice that received (controlFLK-1$^+$+hMSC) spheroids also displayed decreased limb necrosis compared to no treatment group (Figure 6K). However, these mice still showed muscle degeneration and inflammation in the ischemic region (Figures 6I and 6J) and 18.2% of them eventually lost limb (Figure 6K). No statistical difference was observed in fibrotic area between the two groups that received hMSC spheroids or (controlFLK-1$^+$+hMSC) spheroids. In contrast, mice that received (FLK-1$^+$(+DOX)+hMSC) spheroids were protected from limb muscle necrotic damage (Figures 6I and 6J). The majority of the mice that received (FLK-1$^+$(+DOX)+hMSC) spheroids exhibited limb salvage (86.4%) with only mild limb necrosis (9.1%). Only 1 of the 22 mice (4.5%) lost limb (Figure 6K).

Laser Doppler perfusion imaging analysis (Figure 6L) revealed that blood perfusion in ischemic limbs was significantly improved in the group that received (FLK-1$^+$(+DOX)+hMSC) spheroids compared to the other groups. Seven days after treatment, the relative ratios of blood flow (ischemic to normal limb) were 35.6% ± 6.0% in the (FLK-1$^+$(+DOX)+hMSC) spheroid-recipient group compared to the other groups (no treatment, 5.3% ± 2.2%; hMSC spheroid recipients, 13.2% ± 1.8%; controlFLK-1$^+$+hMSC spheroid recipients, 14.4% ± 2.8%; Figure 6L). By day 28, (FLK-1$^+$(+DOX)+hMSC) spheroid-transplanted group significantly improved the relative ratio of blood perfusion (72.6% ± 6.8%) compared to the other groups (no treatment, 3.1% ± 1.7%; hMSC spheroid recipients, 44.6% ± 7.7%; controlFLK-1$^+$+hMSC spheroid recipients, 47.4% ± 5.1%; Figure 6L). No statistical difference was observed between the hMSC spheroid and (controlFLK-1$^+$+hMSC) spheroid transplantation group.

Mice that received (FLK-1$^+$(+DOX)+hMSC) spheroids displayed significantly enhanced CD31$^+$ microvessel formation compared to the other groups (Figures 7A and 7C). SMA-α^+ microvessel formation was also significantly

Figure 6. Enhanced Ischemic Limb Salvage and Vascular Repair by EGS-Induced FLK-1+-hMSC Spheroid Transplantation

(A) CASPASE-3 and Y-chromosome staining from day 3 samples. Apoptotic cells: CASPASE-3 (red), transplanted EGS-induced FLK-1$^+$ cells: Y-chromosome (green), cell nuclei: DAPI (blue), respectively (scale bar = 50 μm). Arrows point to the apoptotic cells derived from EGS-induced FLK-1$^+$ cells.

(B–D) The ratio of CASPASE-3 and Y-chromosome positive cells in the ischemic lesion (*$p < 0.01$, 24 mice/group).

(E) Immunoblot analysis of anti- and proapoptotic factor and angiogenic paracrine factors from day 3 samples.

(F) Quantification of *Bcl-2* and *p53* determined by qRT-PCR (*$p < 0.01$, 24 mice/group).

(G) H&E staining of histological ischemic limb sections 3 days after transplantation (scale bar = 200 μm).

(H) Amount of angiogenic factors produced in ischemic lesion as determined by ELISA (*$p < 0.01$ compared to the FLK-1$^+$(+DOX)+hMSC spheroid group; 24 mice/group).

(I and J) H&E staining (I) and Masson's trichrome staining (J) of histological ischemic limb sections 28 days after treatments (blue indicates fibrosis in [J], scale bar = 200 μm). The asterisk indicates $p < 0.01$ compared to normal group; 22 mice/group.

(K and L) Representative photographs of physiological status (K) and blood perfusion (L) of ischemic hindlimbs. Laser Doppler imaging 0, 7, 14, 21, and 28 days after treatments. All photographs were taken at the same magnification. In (L), $p < 0.01$ compared to no treatment group.

See also Figures S6 and S7 and Table S2.

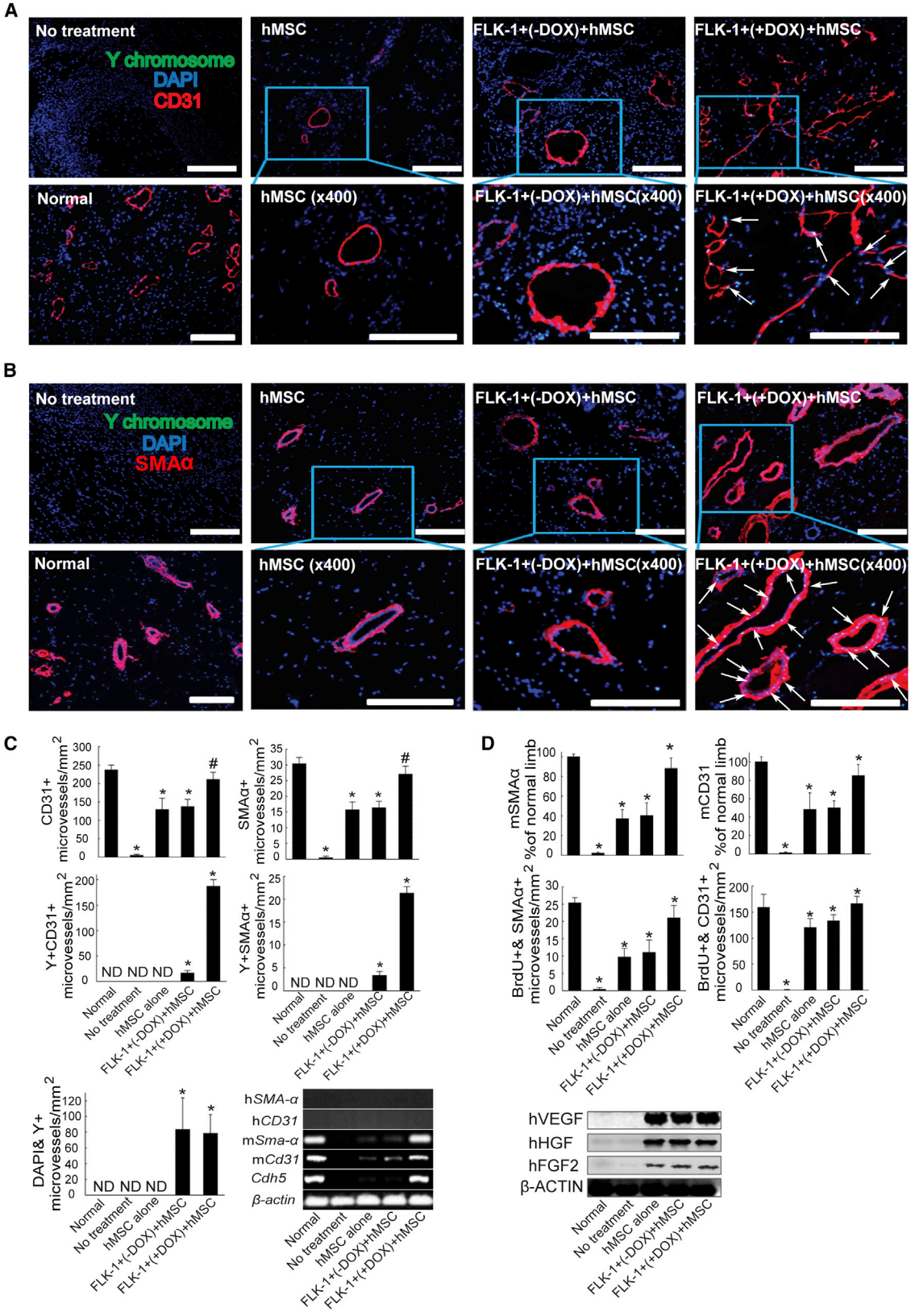

(legend on next page)

enhanced by (FLK-1$^+$(+DOX)+hMSC) spheroid transplantation (Figures 7B and 7C). Significant number of EGS-induced FLK-1$^+$-derived Y$^+$CD31$^+$ (Figures 7A, 7C, and S7A) or Y$^+$SMA-α^+ cells (Figures 7B, 7C, and S7A) were observed in the vasculature. Although a similar number of donor-derived (Y$^+$) cells were detected 28 days after transplantation in mice that received control FLK-1$^+$ or EGS-induced FLK-1$^+$ cells, very few control FLK-1$^+$-derived Y$^+$CD31$^+$ or Y+SMA-α^+ cells were found in the vasculature (Figures 7A–7C). Most of the control FLK-1$^+$ or EGS-induced FLK-1$^+$ progeny cells were found in close proximity to CD31$^+$ or SMA-α^+ microvessels. Many more bromodeoxyuridine (BrdU)-positive microvessels (newly formed microvessels) were detected in limb tissues transplanted with (FLK-1$^+$(+DOX)+hMSC) spheroids compared to the other groups (Figure 7D). While human VEGF, bFGF, and HGF proteins were robustly detected (Figure 7D), human-specific SMA-α or CD31 expression was not detected (Figure 7C), suggesting that the contribution of hMSCs to the vascular repair in all conditions are restricted to paracrine effects.

To determine if therapeutic effect was still observed with reduced cell number of EGS-induced FLK-1$^+$ cells, mice (n = 8 each) were injected with 6 × 10^5 hMSC or (FLK-1$^+$(+DOX)+hMSC) spheroids (1 × 10^5 EGS-induced FLK-1$^+$ cells + 5 × 10^5 hMSCs) after ischemia induction and assessed for their recovery. Compared to the group that received no treatment or hMSC spheroids only, mice that received reduced number of (FLK-1$^+$(+DOX)+hMSC) spheroids still dramatically enhanced angiogenesis, blood flow increase, and limb salvage with reduced muscle degeneration and tissue fibrosis (Figure S6). We also observed abundant Y$^+$CD31$^+$ or Y$^+$SMA-α^+ cells in nascent vessels (Figure S6). This indicated that vascular therapeutic effect could be achieved with as little as 1 × 10^5 EGS-induced FLK-1$^+$ cells.

Finally, we confirmed that EGS-induced FLK-1$^+$ cell outcome was indeed restricted to vessel contribution in noninjury model. Specifically, we injected ESCs or (FLK-1$^+$(+DOX)+hMSC) spheroids subcutaneously into mice. As expected, mice that received ESCs formed distinctive teratomas, which contained multiple tissue types, including cartilage, glands, neuroepithelium, bone, skin, and vessels (Figures S7B and S7D). However, mice transplanted with (FLK-1$^+$(+DOX)+hMSC) spheroids contained only endothelial and smooth muscle cells (Figures S7C and S7D).

DISCUSSION

We transiently coexpressed *Er71*, *Gata2*, and *Scl* during mesoderm formation stage in differentiating ESCs and greatly augmented hemangioblast generation, while near-completely blocking cardiac output. Similarly, we could convert hematopoietic field of the anterior lateral plate mesoderm into cardiac by inhibiting all three hemangiogenic factors in zebrafish. This implies that ER71, GATA2, and SCL form a central core network in hemangioblast development. Enforced ER71, GATA2, and SCL genetic program in ESCs resulted in activation of the BMP-4 and VEGF receptor 2 signaling pathways and inhibition of the PI3K and WNT signaling. Remarkably, each factor contributed uniquely to these signaling pathways, and the collective sum of these was essential for the final hemangioblast outcome.

From the characterizations of enforced *Er71*, *Gata2*, or *Scl* expression in ESCs and the three factor morphants in zebrafish, we propose that ER71 function is upstream of GATA2 and SCL and is required at the commitment stage of hemangioblast generation. GATA2 and SCL maintain the hemangioblast phenotype by suppressing the cardiac program. Indeed, ER71 alone could significantly induce hemangioblasts from ESCs. Moreover, *etsrp* inhibition alone was most powerful in blocking hemangiogenic outcome and converting it into cardiac field in zebrafish. In developing embryos and differentiating ESCs, *Er71* expression is detected prior to *Gata2* and *Scl* expression. Enforced *Er71* expression strongly upregulated *Gata2* and *Scl* expression within 12 hr. On the other hand, enforced *Gata2* or *Scl* expression failed to upregulate *Er71*. Previous studies suggested that *Gata2* and *Scl* are direct targets of ER71 (Kataoka et al., 2011). We also observed ER71 occupancy on the *Scl* promoter region. Recent studies that only the FLK-1$^+$PDGFRα^+ cardiac mesoderm is generated from *Er71*-deficient ESCs (Liu et al., 2012), that vascular endothelial and endocardial progenitors differentiate as

Figure 7. EGS-Induced FLK-1$^+$-Derived Endothelial and Smooth Muscle Cells Are Abundantly Found within Functional Vessels

(A and B) Merged immunofluorescent staining images of Y-chromosome and CD31 (A) or Y and SMAα (B) of ischemic hindlimb tissues 28 days after transplantation. Scale bar indicates 100 μm in low magnification and 70 μm high magnification.

(C) Quantification of CD31 or SMAα-positive microvessel density in the ischemic region and microvessels with Y-chromosome signals ($^*p < 0.01$ and $^\#p < 0.05$ compared to the normal group; 22 mice/group). Human- or mouse-specific gene expression for microvessels were also accessed with RT-PCR.

(D) Newly formed microvessel density was analyzed by BrdU-positive microvessels and relative amount of microvessels in the ischemic lesion. (The asterisk indicates $p < 0.01$ compared to the normal group; 22 mice/group).

See also Figures S6 and S7 and Table S2.

cardiomyocytes in the absence of *etsrp* (Palencia-Desai et al., 2011), and that cardiac program was readily derepressed in *Scl* deficient endothelial cells (Van Handel et al., 2012) support this notion.

We demonstrated that ESC-derived, EGS-induced FLK-1$^+$ hemangioblasts generated functional endothelial and smooth muscle cells in vivo, as demonstrated by CD31+ as well as SMAα^+ vessel structures produced from the EGS-induced FLK-1$^+$ cells in Matrigel plugs. More importantly, we were successful in protecting EGS-induced FLK-1$^+$ cells from apoptosis while preserving their differentiation potential by generating spheroids with hMSCs, which provided survival signal as well as paracrine angiogenic factors. Consequently, EGS-induced FLK-1$^+$-derived endothelial and smooth muscle cells promoted vascular repair and regeneration in a mouse model of hind-limb ischemia. Control FLK-1$^+$ cells were also able to differentiate into functional endothelial and smooth muscle cells. However, they were less efficient in their vascular repair and regeneration potential, probably due to their heterogeneous nature of both cardiac and hemangiogenic potential. Our studies are exciting, as there is great interest in applying stem cell-based therapies for peripheral arterial disease. Clinical trials, phase I and II, have shown that endothelial progenitor cells (EPCs), bone marrow-derived mononuclear cells, MSCs, or the combinations of these cell types are beneficial for patients with limb ischemia or acute myocardial infarction (Katritsis et al., 2005; Lasala et al., 2010, 2012; reviewed in Critser and Yoder, 2010 and Minguell et al., 2013). Moreover, several studies have reported that pluripotent stem-derived mature endothelial cells could improve angiogenic repair and regeneration (Cho et al., 2007; Rufaihah et al., 2011). Currently, however, limitations still exist in applying either pluripotent stem-derived endothelial cells, EPCs, or MSCs clinically. For example, mature endothelial cells have a limited life span. Direct injection of ESC-derived endothelial cells into damaged ischemic area in animal models has met with limited success, due to apoptosis resulting in limited engraftment. We envision that ESC-derived FLK-1$^+$ vascular progenitors would be ideal for future therapeutic applications in peripheral arterial disease. The current strategy of EGS-induced FLK-1$^+$ cell delivery with MSCs as vascular tissue spheroids could also be extended to additional cell types, including EPCs and bone marrow mononuclear cells.

In summary, we developed a powerful strategy generating hemangiogenic FLK-1$^+$ progenitors from ESCs. The unlimited access to hemangioblasts, the ultimate hematopoietic and vascular progenitors, warrants further investigations on potential clinical applications requiring hematopoietic, vascular repair and regeneration. In the future, however, a strategy of deleting the exogenous genes after hemangioblast induction should be considered. Derivation and future applications of hemangioblasts from human pluripotent stem cells in peripheral arterial diseases are warranted.

EXPERIMENTAL PROCEDURES

ESC Generation

Er71$^{+/+}$ and *Er71*$^{-/-}$ ESC lines and inducible ESC lines (*iEr71* and *iGata2)* were generated as described previously (Lee et al., 2008; Liu et al., 2012; Lugus et al., 2007). Inducible *Scl* or *Er71-2A-Gata2-2A-Scl* (*iEGS*) ESCs were generated by targeting the tet-responsive locus of A2Lox cells (Ismailoglu et al., 2008), with the construct containing the coding sequence of *Scl* or *Er71, Gata2,* and *Scl*, which were linked by 2A peptides (de Felipe, 2002). *Scl* was fused to a Flag tag at the 3′ end. After the correct targeting event was confirmed by a tet-responsive locus/complementary DNA vector-specific PCR, inducible *Scl* or *Er71, Gata2,* and *Scl* expression with 1 μg/ml DOX was verified by RNA and Immunoblot analyses.

Microarray and Pathway Enrichment Analysis

Global gene expression profiles were analyzed using the GeneChip Mouse Gene 1.0 ST arrays (Affymetrix). Data were normalized, and expression values were modeled with Partek Genomics Suite (Partek). Differentially expressed genes were determined with significant p value < 0.05 and false discovery rate < 0.25. Raw data are available at the Gene Expression Omnibus repository (accession number GSE45147). Based on the microarray data, pathway enrichment analysis and interaction networks building were performed using MetaCore Analytical Suite (GeneGo).

Mouse Hindlimb Ischemia

Hindlimb ischemia was induced in mice as previously described (Shim et al., 2012). Four-week-old female athymic mice (20–25 g body weight; Jackson Laboratory) were anesthetized with xylazine (10 mg/kg) and ketamine (100 mg/kg). The femoral artery and its branches were ligated via skin incision using a 6-0 silk suture (Ethicon), along with the external iliac artery and all upstream arteries. The femoral artery was then excised from its proximal origin as a branch of the external iliac artery to the distal point, whereupon it bifurcates into the saphenous and popliteal arteries. All animals received humane care (Institutional Animal Care and Use Committee No. 20110260).

Transplantation of FLK-1$^+$(+DOX)+hMSC Spheroids into Ischemic Mouse Hindlimbs

Mice were randomly divided into five groups (n = 22 from three independent experiments). Normal mice that did not undergo any surgery or mice with surgery but without treatment were used as controls. hMSC, controlFLK-1$^+$+hMSC or FLK-1$^+$(+DOX)+hMSC spheroids (3×10^4 cells/spheroid; 100 spheroids/limb; total 3×10^6 cells/limb; 0.5×10^6 EGS-induced FLK-1$^+$ cells + 2.5×10^6 hMSC cells/limb) were intramuscularly injected into the gracilis muscle of the medial thigh.

Laser Doppler Imaging Analysis

Laser Doppler imaging analysis was performed as described previously (Shim et al., 2012). A laser Doppler perfusion imager (Moor Instruments) was used for serial noninvasive physiological evaluation of neovascularization. Mice were monitored by serial scanning of surface blood flow in hindlimbs at days 0, 7, 14, 21, and 28. Digital color-coded images were scanned and analyzed to quantify a blood flow in ischemic regions from the knee joint to the toe. Mean values of perfusion were subsequently calculated. The morphological status of the ischemic limb was monitored for 4 weeks.

Statistical Analysis

The results of qRT-PCR and flow cytometry analysis were analyzed by Student's t test or one-way ANOVA (four group comparisons) with a Bonferroni multiple comparison posttest (GraphPad software). A p value <0.05 was considered significant.

SUPPLEMENTAL INFORMATION

Supplemental Information includes Supplemental Experimental Procedures, seven figures, and four tables and can be found with this article online at http://dx.doi.org/10.1016/j.stemcr.2013.06.005.

ACKNOWLEDGMENTS

We thank the Cell Sorter Cores of the Alvin J. Siteman Cancer Center (supported in part by an NCI Cancer Centre Support Grant No. P30 CA91842) and the Department of Pathology and Immunology at the Washington University School of Medicine. This work was supported by grants from American Heart Association Postdoctoral Fellowship 10POST4570022 (to F.L.) and National Institutes of Health grants HL63736 and HL55337 (to K.C.).

Received: January 16, 2013
Revised: June 13, 2013
Accepted: June 17, 2013
Published: July 25, 2013

REFERENCES

Bhang, S.H., Lee, S., Shin, J.Y., Lee, T.J., and Kim, B.S. (2012). Transplantation of cord blood mesenchymal stem cells as spheroids enhances vascularization. Tissue Eng. Part A *18*, 2138–2147.

Caprioli, A., Koyano-Nakagawa, N., Iacovino, M., Shi, X., Ferdous, A., Harvey, R.P., Olson, E.N., Kyba, M., and Garry, D.J. (2011). Nkx2-5 represses Gata1 gene expression and modulates the cellular fate of cardiac progenitors during embryogenesis. Circulation *123*, 1633–1641.

Cho, S.W., Moon, S.H., Lee, S.H., Kang, S.W., Kim, J., Lim, J.M., Kim, H.S., Kim, B.S., and Chung, H.M. (2007). Improvement of postnatal neovascularization by human embryonic stem cell derived endothelial-like cell transplantation in a mouse model of hindlimb ischemia. Circulation *116*, 2409–2419.

Choi, K., Kennedy, M., Kazarov, A., Papadimitriou, J.C., and Keller, G. (1998). A common precursor for hematopoietic and endothelial cells. Development *125*, 725–732.

Chung, Y.S., Zhang, W.J., Arentson, E., Kingsley, P.D., Palis, J., and Choi, K. (2002). Lineage analysis of the hemangioblast as defined by FLK1 and SCL expression. Development *129*, 5511–5520.

Critser, P.J., and Yoder, M.C. (2010). Endothelial colony-forming cell role in neoangiogenesis and tissue repair. Curr. Opin. Organ Transplant. *15*, 68–72.

de Felipe, P. (2002). Polycistronic viral vectors. Curr. Gene Ther. *2*, 355–378.

Ema, M., Faloon, P., Zhang, W.J., Hirashima, M., Reid, T., Stanford, W.L., Orkin, S., Choi, K., and Rossant, J. (2003). Combinatorial effects of Flk1 and Tal1 on vascular and hematopoietic development in the mouse. Genes Dev. *17*, 380–393.

Faloon, P., Arentson, E., Kazarov, A., Deng, C.X., Porcher, C., Orkin, S., and Choi, K. (2000). Basic fibroblast growth factor positively regulates hematopoietic development. Development *127*, 1931–1941.

Huber, T.L., Kouskoff, V., Fehling, H.J., Palis, J., and Keller, G. (2004). Haemangioblast commitment is initiated in the primitive streak of the mouse embryo. Nature *432*, 625–630.

Ismailoglu, I., Yeamans, G., Daley, G.Q., Perlingeiro, R.C., and Kyba, M. (2008). Mesodermal patterning activity of SCL. Exp. Hematol. *36*, 1593–1603.

Kataoka, H., Hayashi, M., Nakagawa, R., Tanaka, Y., Izumi, N., Nishikawa, S., Jakt, M.L., Tarui, H., and Nishikawa, S. (2011). Etv2/ER71 induces vascular mesoderm from Flk1+PDGFRα+ primitive mesoderm. Blood *118*, 6975–6986.

Katritsis, D.G., Sotiropoulou, P.A., Karvouni, E., Karabinos, I., Korovesis, S., Perez, S.A., Voridis, E.M., and Papamichail, M. (2005). Transcoronary transplantation of autologous mesenchymal stem cells and endothelial progenitors into infarcted human myocardium. Catheter. Cardiovasc. Interv. *65*, 321–329.

Kattman, S.J., Huber, T.L., and Keller, G.M. (2006). Multipotent flk-1+ cardiovascular progenitor cells give rise to the cardiomyocyte, endothelial, and vascular smooth muscle lineages. Dev. Cell *11*, 723–732.

Kattman, S.J., Witty, A.D., Gagliardi, M., Dubois, N.C., Niapour, M., Hotta, A., Ellis, J., and Keller, G. (2011). Stage-specific optimization of activin/nodal and BMP signaling promotes cardiac differentiation of mouse and human pluripotent stem cell lines. Cell Stem Cell *8*, 228–240.

Kennedy, M., D'Souza, S.L., Lynch-Kattman, M., Schwantz, S., and Keller, G. (2007). Development of the hemangioblast defines the onset of hematopoiesis in human ES cell differentiation cultures. Blood *109*, 2679–2687.

Koyano-Nakagawa, N., Kweon, J., Iacovino, M., Shi, X., Rasmussen, T.L., Borges, L., Zirbes, K.M., Li, T., Perlingeiro, R.C., Kyba, M., and Garry, D.J. (2012). Etv2 is expressed in the yolk sac hematopoietic and endothelial progenitors and regulates Lmo2 gene expression. Stem Cells *30*, 1611–1623.

Lasala, G.P., Silva, J.A., Gardner, P.A., and Minguell, J.J. (2010). Combination stem cell therapy for the treatment of severe limb ischemia: safety and efficacy analysis. Angiology *61*, 551–556.

Lasala, G.P., Silva, J.A., and Minguell, J.J. (2012). Therapeutic angiogenesis in patients with severe limb ischemia by transplantation of a combination stem cell product. J. Thorac. Cardiovasc. Surg. *144*, 377–382.

Lee, D., Park, C., Lee, H., Lugus, J.J., Kim, S.H., Arentson, E., Chung, Y.S., Gomez, G., Kyba, M., Lin, S., et al. (2008). ER71 acts downstream of BMP, Notch, and Wnt signaling in blood and vessel progenitor specification. Cell Stem Cell *2*, 497–507.

Lindsley, R.C., Gill, J.G., Murphy, T.L., Langer, E.M., Cai, M., Mashayekhi, M., Wang, W., Niwa, N., Nerbonne, J.M., Kyba, M., and Murphy, K.M. (2008). Mesp1 coordinately regulates cardiovascular fate restriction and epithelial-mesenchymal transition in differentiating ESCs. Cell Stem Cell *3*, 55–68.

Liu, F., Walmsley, M., Rodaway, A., and Patient, R. (2008). Fli1 acts at the top of the transcriptional network driving blood and endothelial development. Curr. Biol. *18*, 1234–1240.

Liu, F., Kang, I., Park, C., Chang, L.W., Wang, W., Lee, D., Lim, D.S., Vittet, D., Nerbonne, J.M., and Choi, K. (2012). ER71 specifies Flk-1+ hemangiogenic mesoderm by inhibiting cardiac mesoderm and Wnt signaling. Blood *119*, 3295–3305.

Lugus, J.J., Chung, Y.S., Mills, J.C., Kim, S.I., Grass, J., Kyba, M., Doherty, J.M., Bresnick, E.H., and Choi, K. (2007). GATA2 functions at multiple steps in hemangioblast development and differentiation. Development *134*, 393–405.

Lugus, J.J., Park, C., Ma, Y.D., and Choi, K. (2009). Both primitive and definitive blood cells are derived from Flk-1+ mesoderm. Blood *113*, 563–566.

Minguell, J.J., Allers, C., and Lasala, G.P. (2013). Mesenchymal stem cells and the treatment of conditions and diseases: the less glittering side of a conspicuous stem cell for basic research. Stem Cells Dev. *22*, 193–203.

Moretti, A., Caron, L., Nakano, A., Lam, J.T., Bernshausen, A., Chen, Y., Qyang, Y., Bu, L., Sasaki, M., Martin-Puig, S., et al. (2006). Multipotent embryonic isl1+ progenitor cells lead to cardiac, smooth muscle, and endothelial cell diversification. Cell *127*, 1151–1165.

Motoike, T., Markham, D.W., Rossant, J., and Sato, T.N. (2003). Evidence for novel fate of Flk1+ progenitor: contribution to muscle lineage. Genesis *35*, 153–159.

Palencia-Desai, S., Kohli, V., Kang, J., Chi, N.C., Black, B.L., and Sumanas, S. (2011). Vascular endothelial and endocardial progenitors differentiate as cardiomyocytes in the absence of Etsrp/Etv2 function. Development *138*, 4721–4732.

Pham, V.N., Lawson, N.D., Mugford, J.W., Dye, L., Castranova, D., Lo, B., and Weinstein, B.M. (2007). Combinatorial function of ETS transcription factors in the developing vasculature. Dev Biol *303*, 772–783.

Rufaihah, A.J., Huang, N.F., Jamé, S., Lee, J.C., Nguyen, H.N., Byers, B., De, A., Okogbaa, J., Rollins, M., Reijo-Pera, R., et al. (2011). Endothelial cells derived from human iPSCS increase capillary density and improve perfusion in a mouse model of peripheral arterial disease. Arterioscler. Thromb. Vasc. Biol. *31*, e72–e79.

Schoenebeck, J.J., Keegan, B.R., and Yelon, D. (2007). Vessel and blood specification override cardiac potential in anterior mesoderm. Dev. Cell *13*, 254–267.

Shim, M.S., Bhang, S.H., Yoon, K., Choi, K., and Xia, Y. (2012). A bioreducible polymer for efficient delivery of Fas-silencing siRNA into stem cell spheroids and enhanced therapeutic angiogenesis. Angew. Chem. Int. Ed. Engl. *51*, 11899–11903.

Van Handel, B., Montel-Hagen, A., Sasidharan, R., Nakano, H., Ferrari, R., Boogerd, C.J., Schredelseker, J., Wang, Y., Hunter, S., Org, T., et al. (2012). Scl represses cardiomyogenesis in prospective hemogenic endothelium and endocardium. Cell *150*, 590–605.

Yamashita, J., Itoh, H., Hirashima, M., Ogawa, M., Nishikawa, S., Yurugi, T., Naito, M., Nakao, K., and Nishikawa, S. (2000). Flk1-positive cells derived from embryonic stem cells serve as vascular progenitors. Nature *408*, 92–96.

Yang, L., Soonpaa, M.H., Adler, E.D., Roepke, T.K., Kattman, S.J., Kennedy, M., Henckaerts, E., Bonham, K., Abbott, G.W., Linden, R.M., et al. (2008). Human cardiovascular progenitor cells develop from a KDR+ embryonic-stem-cell-derived population. Nature *453*, 524–528.